Real time monitoring of the *in situ* growth of silver nanoparticles in a polymer film under ambient conditions†

G. V. Ramesh,[a] B. Sreedhar[b] and T. P. Radhakrishnan*[a]

Received 13th July 2009, Accepted 21st August 2009
First published as an Advance Article on the web 11th September 2009
DOI: 10.1039/b913931a

Direct monitoring of the formation and growth of nanoparticles by microscopy in real time is of fundamental interest in understanding the chemical and self assembly processes involved. Such studies are difficult to implement in solution, but have been carried out on solid substrates, mostly under specialized conditions, including ultra high vacuum. The present study illustrates the facility with which *in situ* growth of metal nanoparticles in thin polymer films under ambient conditions can be monitored by real time atomic force microscopy. Formation of silver nanoparticles inside spin-coated thin films of poly(vinylpyrrolidone) containing silver nitrate, under ambient conditions, is revealed by the emergence and growth of surface plasmon resonance absorption extending over several hours. Atomic force microscopy allows 'direct observation' of structures growing near the surface; individual nanostructures can be monitored in the case of very thin films. A plausible mechanism is proposed for the chemical reactions occurring inside the film with the polymer itself acting as the reducing agent leading to the formation and growth of the nanoparticles. The present study opens up new avenues to carry out investigations into the mechanisms and kinetics of nanoparticle growth.

1. Introduction

Investigations of metal nanoparticles have largely addressed the development of fabrication and assembly protocols, exploration of novel and unique characteristics and realization of a plethora of applications. The temporal evolution during their formation especially *via* 'bottom-up' approaches is a fundamental issue. During solution phase synthesis, perhaps the most popular route used, the time course of the growth can be followed spectroscopically or by imaging samples removed periodically from the reaction medium with the growth arrested; monitoring of the nanostructures *via* direct real time microscopy is difficult. Investigations of the latter kind have been carried out under specialized conditions. Nucleation and growth of gold nanoparticles on a reduced titania surface followed by their chemical/thermal treatment were explored by *in situ* scanning tunneling microscopy.[1] The growth of cobalt nuclei on a boron-doped diamond electrode under potentiostatic conditions has been investigated by *in situ* atomic force microscopy (AFM).[2] Investigations on non-metal systems include transmission electron microscopy (TEM) imaging of electron beam-induced changes in iron oxide nanoparticles and evolution of silicon nanowires formed by laser ablation,[3] as well as an ultra high vacuum TEM study of the nucleation kinetics of silicon particles formed from a gold–silicon eutectic.[4]

Thin polymer films with embedded metal nanoparticles are versatile composite materials combining the unique properties of nanoparticles and polymers, often synergistically. Among the various approaches to their fabrication, *in situ* methods wherein the nanoparticles are generated within the polymer film by thermal/photochemical reduction or decomposition of precursors, are simple and efficient;[5] deployment of the polymer itself as the reducing and stabilizing agent is particularly attractive.[6] The environmentally benign protocol that we have optimized for the fabrication of noble metal nanoparticle-embedded poly(vinyl alcohol) (PVA) film[7–9] provides free-standing and supported films with a range of applications,[7,10,11] and enables the analysis of the chemistry occurring inside the film.[8,9] We visualized that the *in situ* growth of metal nanoparticles in thin polymer films offers a unique opportunity to 'see' the growth of nanostructures in real time using microscopy. It would be singularly interesting if the growth was to occur spontaneously under ambient conditions.

Poly(vinylpyrrolidone) (PVP) is most popular as a stabilizer for nanoparticles, however it can also act as the reducing agent in the formation of metal nanoparticles.[12–15] $HAuCl_4$ is reduced to gold nanoparticles by PVP in aqueous solution even at 25 °C, whereas the reduction of $AgNO_3$ is more sluggish.[12] Interestingly, we observed that Ag^+ undergoes reduction to Ag inside PVP thin film under ambient temperature and atmospheric conditions. We note that, fabrication of Ag and Au nanoparticles in films of various polymers including PVP by the *in situ* method[6,7] has been reported very recently;[16] in this study, low molecular weight PVP was employed and the film was baked at 220 °C, well above its glass transition temperature. Below, we describe the real time monitoring of the growth of silver nanoparticles in PVP films under ambient

---

[a] *School of Chemistry, University of Hyderabad, Hyderabad – 500046, India. E-mail: tprsc@uohyd.ernet.in; Fax: 91-40-2301-2460; Tel: 91-40-2313-4827*
[b] *Inorganic and Physical Chemistry Division, Indian Institute of Chemical Technology, Hyderabad – 500 607, India*

† Electronic supplementary information (ESI) available: Details of spectroscopy and microscopy (including a movie of the real time growth), and control experiments. See DOI: 10.1039/b913931a

conditions, using spectroscopy and microscopy. We discuss a plausible mechanism involved in this process.

2. Experimental

20.0 mg PVP (Aldrich, average molecular weight = 1300 kDa) was dissolved in 2.0 ml of 0.095 M aqueous solution of $AgNO_3$ to yield a mixture with a Ag/PVP weight ratio, x = 1.0 (cases with x = 0.5 and 0.25 are discussed briefly in the ESI†). In order to prepare very thin films, the solution was diluted further by adding 0.4 ml water. The solution was stirred for 5 min under ambient temperature (~25 °C), protecting it from light. MilliQ purified water was used in all operations. Glass plates used as substrates were cleaned by soap solution and water followed by sonication in acetone for 10 min. They were finally sonicated in isopropyl alcohol for 10 min and dried. Mica sheets cleaved to expose fresh surface were also used as substrates.

The $AgNO_3$–PVP solution was spin-coated on the substrate using a Laurell Technologies Corporation Model WS-400B-6NPP/LITE/8K Photoresist Spinner operated at 500 RPM for 10 s followed by 4000 RPM for 10 s. The films were dried by blowing dry nitrogen gas for 3 min. Films coated on glass were used for electronic absorption spectroscopy and AFM studies. Films coated on mica substrates were also examined using AFM. Substrates for films used in TEM imaging were prepared following the procedure we have developed earlier.[7] A few drops of a solution of polystyrene (average molecular weight = 280 kDa) in toluene (1 g in 8 ml) was spin-coated on glass at 1000 RPM for 10 s and dried in a hot air oven at 90 °C for 10–15 min. The $AgNO_3$–PVP solution was spin-coated on the polystyrene film and dried by blowing dry nitrogen gas for 3 min. This plate was dipped in toluene to dissolve the polystyrene layer; the $AgNO_3$–PVP film that came free was collected on a 200-mesh copper grid for TEM imaging. Alternately, the $AgNO_3$–PVP solution was spin-coated directly on carbon supported copper grid held on a glass plate.

The thickness of the films was measured using an Ambios Technology XP-1 profilometer. Electronic absorption spectra of the films coated on glass substrates were recorded on a Cary 100 Bio UV-Visible Spectrophotometer. Growth of the nanoparticles in the film was observed in real time using a SEIKO Model SPA400 AFM operated in dynamic force mode with a cantilever having force constant of 12 N m^{-1}. Grain size and surface analysis were carried out using SPIWin Version 3.01 provided by the manufacturer of the AFM. TEM imaging was done in TECNAI G^2 FEI F12 microscope at an accelerating voltage of 120 kV.

3. Results and discussion

As observed in solution studies reported earlier,[12,13] we found that the reduction of $AgNO_3$ to Ag is more facile with lower molecular weight PVP in the case of thin films as well. In spite of the slower reaction rate, we chose PVP with a relatively high molecular weight because of the good quality films it provided. As discussed above, all film fabrication procedures were carried out in air, under ambient conditions. Observation of the distinct SPR absorption within an hour of fabrication of the film indicated the formation of silver nanoparticles. The increasing intensity of the absorption (Fig. 1) suggests that the nanoparticle formation continues for several hours; the red shift points to the increasing average size of particles. Formation and growth of the particles appear to slow down after ~24 h. It may be noted that the spectra of samples kept in the dark for different time periods were identical to that of films exposed for the same time, ruling out any significant role of photochemical processes.

Growth of the nanoparticles near the surface of films, typically 40 nm thick coated on glass substrates, was monitored in real time using AFM. A fixed area, typically 2 × 2 μm^2, was scanned at regular time intervals for several hours without disturbing the sample. Small drifts of the scan area do occur over such long periods. Therefore, images of a specific region were carefully selected by making use of some permanent marks on the film and clipped; a typical set of images is shown in Fig. 2 (a more extensive set is provided in the ESI†). It may be noted that in this and some of the later AFM images, the z-axis scale is expanded considerably compared to the x- and y-axes. Starting with a plain polymer

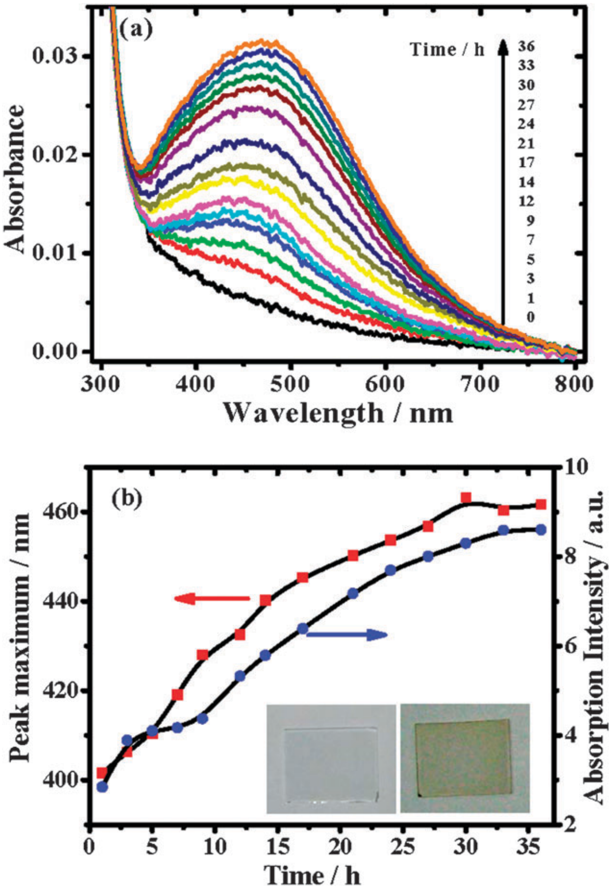

Fig. 1 (a) Electronic absorption spectra of Ag–PVP film on glass, under ambient conditions recorded in real time; time elapsed after the first recording (~5 min after fabrication) is indicated; (b) plot of the plasmon absorption peak maximum and its integrated absorption intensity (see ESI†) *versus* time (inset shows photographs of a fresh film (left, colorless) and one kept in the dark for 72 h (right, yellow)).

surface, a uniform growth of nanostructures is clearly evident. We have observed similar effects in films coated on mica, ruling out any specific substrate effects. The growth of nanostructures observed can be attributed to silver nanoparticles forming close to the surface of the film, as control experiments using pure PVP films showed no morphology changes in the AFM images for up to 24 h (see ESI†).

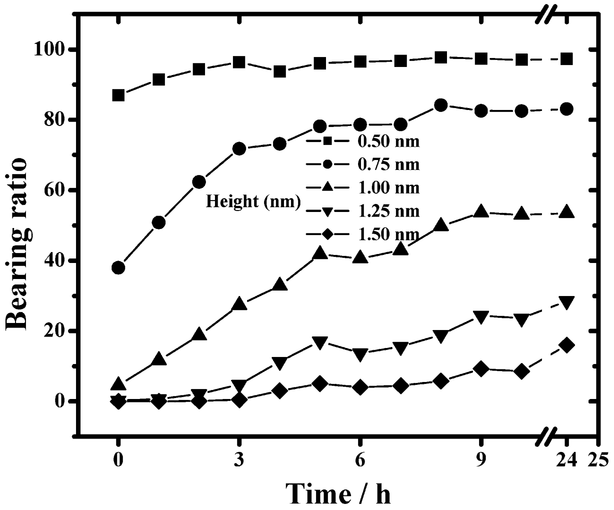

Fig. 3 Plot of bearing ratios at different heights in AFM images (selected ones shown in Fig. 2) of the Ag-PVP film as a function of time elapsed after the first imaging.

We have carried out grain size analysis of the images in order to construct a profile of the growth (Fig. 2, last panel). For each image, the grain size distribution was examined at different height thresholds from 0.7 to 3.1 nm at intervals of 0.1 nm; the lower limit was set by the level above which the nanostructures are clearly visible against the background of the polymer and the upper limit by the highest level to which the nanostructures are found to grow in the film. A plot of the height *versus* mean radius was constructed and a mirror image of this plot about the *y*-axis was added. With an additional point introduced arbitrarily at 0.1 nm above the highest points to connect the two curves, a quantitative representation of the average dimensions of the nanostructures in an image is obtained. Collection of such plots constructed from the images (Fig. 2) provides a profile of the nanostructure growth near the surface. The bearing ratios determined from surface analysis signify the percentage of data points at or above any specified height level in the image and ranges from 0 at the highest point in the image to 100 at the substrate level. Plots of the bearing ratios at different height levels as a function of time indicate clearly the increase in the number of growing particles (Fig. 3). View of contiguous frames (see the movie file in the ESI†) of the AFM images reveals occasional, minor downward shift of a few nanostructures in the neighborhood of an emerging or

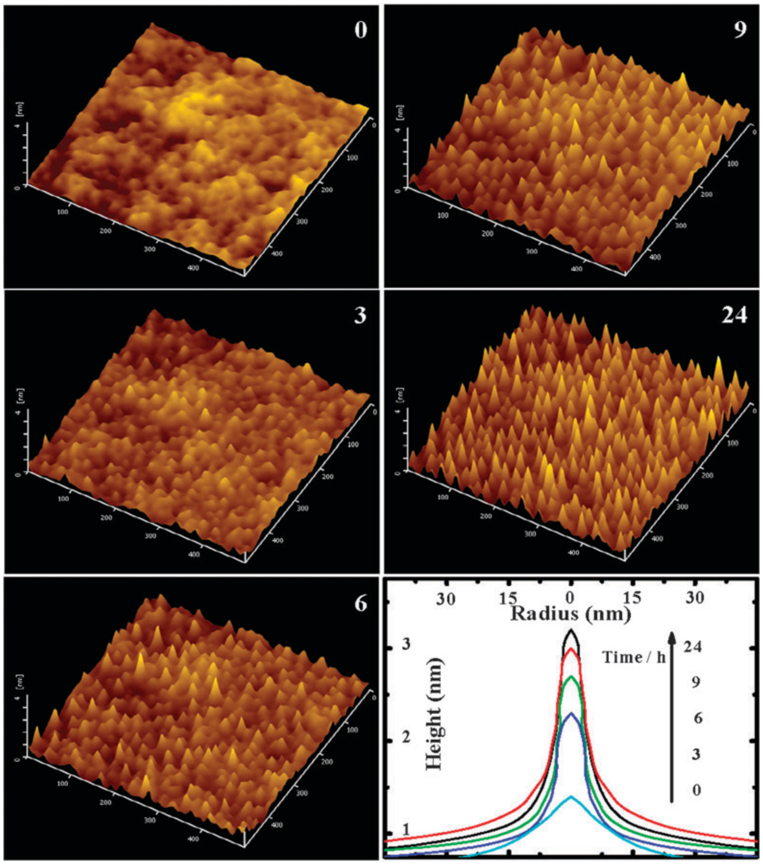

Fig. 2 Real time AFM images (0.5 μm × 0.5 μm × 4 nm) of the growth of nanostructures in Ag–PVP film; time in hours elapsed after the first imaging (~15 min after fabrication) is shown. The last panel is a schematic representation of the growth, using average height and radius (see text for details).

growing one; these possibly indicate local reorganizations within the polymer matrix accompanying the growth. None of the AFM observations show any sign of rupture of the polymer film during the nanoparticle growth; the relatively small heights to which the particles grow and the elasticity of the polymer film probably preclude this.

Careful search with thinner (~25 nm) films fabricated from more dilute solutions, allowed us to observe relatively larger and well separated structures and monitor the growth of individual ones within the first hour itself (Fig. 4). These structures result from local aggregation of silver atoms inside the film. A single structure in the images in Fig. 4 was clipped and subjected to grain size analysis. The profile of each of the structures observed above the film surface indicate that the relevant particle is approximately spherical (see ESI†). The height and diameter at half-height of the structure as a function of time is plotted in Fig. 5; it provides a description of the growth of that nanostructure. Fig. 4 also reveals the emergence of new structures during the growth of others. These are likely to be particles growing from deeper inside the film.

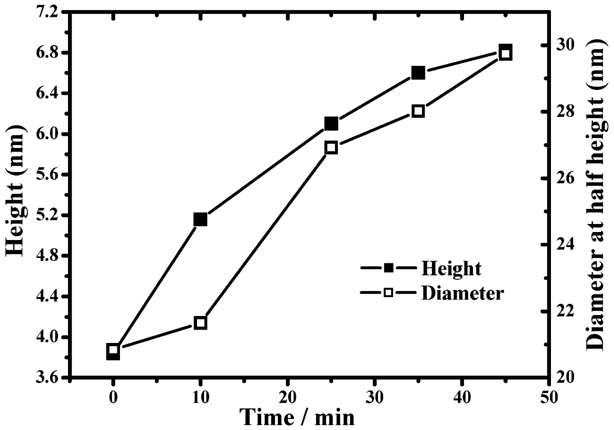

Fig. 5 Plot of the height and diameter (at half height) of the single nanostructure shown in Fig. 4 as a function of time elapsed after the first imaging; the line is only a guide to the eye.

Films maintained under ambient conditions in the dark for 24 h were imaged using TEM. Fig. 6 shows the uniform distribution of silver nanoparticles in the range 2–5 nm and

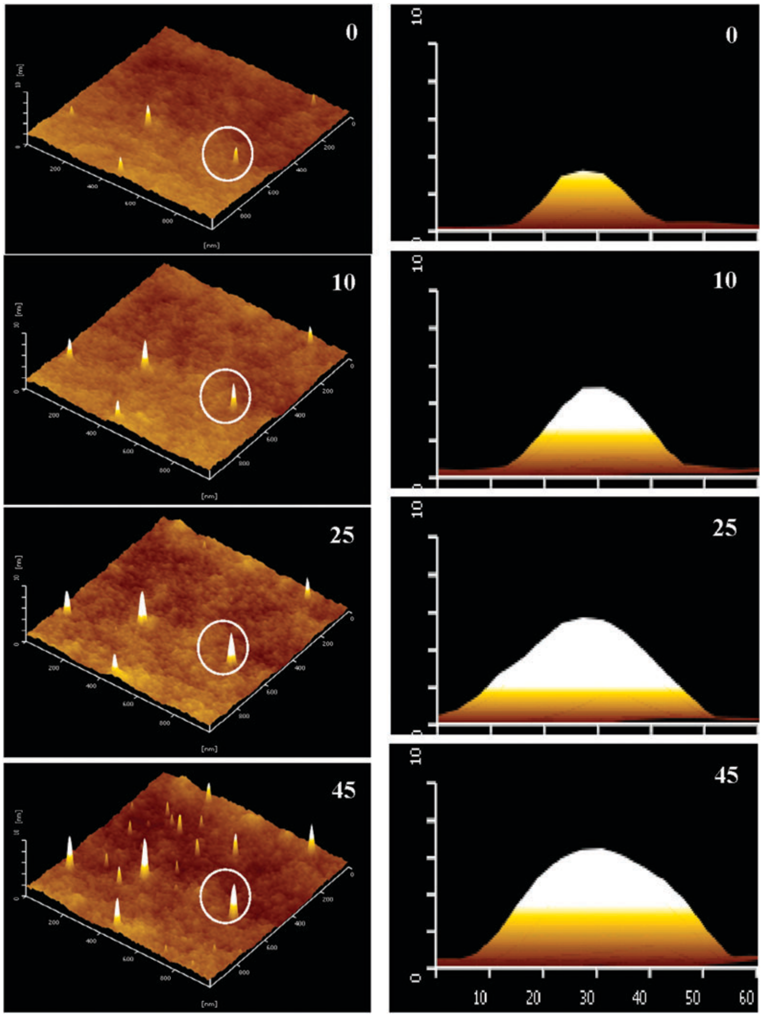

Fig. 4 Left: real time AFM images (1 μm × 1 μm × 10 nm) of the growth of nanostructures in thin Ag-PVP film; time in minutes elapsed after the first imaging (~15 min after fabrication) is shown. Right: magnified 2D view (60 × 10 nm^2) of the structure encircled in the left panel.

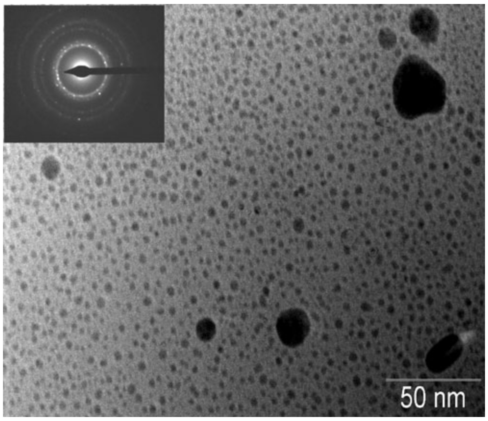

Fig. 6 TEM image of Ag–PVP film maintained under ambient conditions in the dark for 24 h after fabrication; electron diffraction pattern is shown in the inset.

infrequent occurrence of larger ($\sim$15–30 nm) particles. Based on these observations, we conclude that the nanostructures distributed homogeneously in the images in Fig. 2 with average diameter of $\sim$20 nm and heights typically below 3–4 nm are likely to be collections of a few nanoparticles wrapped by the polymer and that the structures in the images in Fig. 4 correspond to the isolated large particles. As noted above, analysis of the shape and geometry of the features observed in the AFM images suggests that the latter conform to segments of growing single spheres, whereas those in the former are more complex. Structural changes in the polymer matrix also contributing to the evolution of the film morphology cannot be ruled out.

We have carried out some control experiments to gain insight into the mechanism of formation of silver nanoparticles inside the PVP film (see ESI†). Interestingly, unlike $AgNO_3$, $HAuCl_4$ is not reduced inside the PVP film even upon heating. This suggests that an initial step involving the complexation of the metal cation with the carbonyl groups of PVP is likely. This picture is supported by our observation that incorporation of Zn^{2+} ions hinders the formation of silver nanoparticles in the film, possibly due to the efficient binding of Zn^{2+} to the amide groups.[17] This mechanistic step is similar to the coordination of Ag^+ ions with the oxygen atoms in PVA film proposed earlier.[18] We have also observed that metal nanoparticles are not formed on treating $AgNO_3$ or $HAuCl_4$ with *N*-methylpyrrolidone in solution, reinforcing the view expressed earlier[12] that dehydrogenation of the PVP backbone is involved in the metal ion reduction. The tentative mechanism that can be proposed, based on these control experiments and observations, involves binding of the Ag^+ ions to the carbonyl group of PVP and subsequent reduction effected by dehydrogenation of the carbon chain (see ESI†). Silver atoms formed within close proximity of each other are likely to diffuse inside the polymer matrix, nucleate and grow into nanocrystals.

4. Conclusions

The present study illustrates a case of *in situ* growth of silver nanoparticles inside a polymer film under ambient conditions and the convenient monitoring of the particle growth in real time by spectroscopy and AFM imaging. Observations we have made in preliminary studies of Au-PVA films, point to the feasibility of extending similar investigations to other systems. Real time monitoring should facilitate investigations into the kinetics and mechanisms of the growth of nanostructures in polymer films.

Acknowledgements

Financial support from the DST, New Delhi, infrastructure support from the Centre for Nanotechnology at the University of Hyderabad and a senior research fellowship for GVR from CSIR, New Delhi are acknowledged.

References

1 A. Kolmakov and D. W. Goodman, *Chem. Rec.*, 2002, **2**, 446.
2 A. O. Simm, X. Ji, C. E. Banks, M. E. Hyde and R. G. Compton, *ChemPhysChem*, 2006, **7**, 704.
3 (*a*) A. H. Latham, M. J. Wilson, P. Schiffer and M. E. Williams, *J. Am. Chem. Soc.*, 2006, **128**, 12632; (*b*) M. L. Taheri, B. W. Reed, T. B. La Grange and N. D. Browning, *Small*, 2008, **4**, 2187.
4 B. J. Kim, J. Tersoff, S. Kodambaka, M. C. Reuter, E. A. Stach and F. M. Ross, *Science*, 2008, **322**, 1070.
5 (*a*) A. S. Korchev, M. J. Bozack, B. L. Slaten and G. Mills, *J. Am. Chem. Soc.*, 2004, **126**, 10; (*b*) S. Rifai, C. A. Breen, D. J. Solis and T. M. Swager, *Chem. Mater.*, 2006, **18**, 21; (*c*) J. Zhang, Y. Gao, R. A. Alvarez-Puebla, J. M. Buriak and H. Fenniri, *Adv. Mater.*, 2006, **18**, 3233; (*d*) J. Li, K. Kamata, S. Watanabe and T. Iyoda, *Adv. Mater.*, 2007, **19**, 1267; (*e*) M. Sakamoto, T. Tachikawa, M. Fujitsuka and T. Majima, *Adv. Funct. Mater.*, 2007, **17**, 857; (*f*) R. D. Deshmukh and R. J. Composto, *Chem. Mater.*, 2007, **19**, 745; (*g*) L. Shang, Y. Wang, L. Huang and S. Dong, *Langmuir*, 2007, **23**, 7738; (*h*) T. Hasell, L. Lagonigro, A. C. Peacock, S. Yoda, P. D. Brown, P. J. A. Sazio and S. M. Howdle, *Adv. Funct. Mater.*, 2008, **18**, 1265.
6 W. Fritzsche, H. Porwol, A. Wiegand, S. Bornmann and J. M. Köhler, *Nanostruct. Mater.*, 1998, **10**, 89.
7 (*a*) S. Porel, S. Singh, S. S. Harsha, D. N. Rao and T. P. Radhakrishnan, *Chem. Mater.*, 2005, **17**, 9; (*b*) G. V. Ramesh, S. Porel and T. P. Radhakrishnan, *Chem. Soc. Rev.*, 2009, **38**, 2646.
8 S. Porel, S. Singh and T. P. Radhakrishnan, *Chem. Commun.*, 2005, 2387.
9 S. Porel, N. Hebalkar, B. Sreedhar and T. P. Radhakrishnan, *Adv. Funct. Mater.*, 2007, **17**, 2550.
10 S. Porel, N. Venkatram, D. N. Rao and T. P. Radhakrishnan, *J. Appl. Phys.*, 2007, **102**, 033107.
11 (*a*) X. Meng, K. Fujita, Y. Zong, S. Murai and K. Tanaka, *Appl. Phys. Lett.*, 2008, **92**, 201112; (*b*) R. Abargues, J. Marqués-Hueso, J. Canet-Ferrer, E. Pedrueza, J. L. Valdés, E. Jiménez and J. P. Martínez-Pastor, *Nanotechnology*, 2008, **19**, 355308.
12 C. E. Hoppe, M. Lazzari, I. Pardiñas-Blanco and M. A. López-Quintela, *Langmuir*, 2006, **22**, 7027.
13 I. Washio, Y. Xiong, Y. Yin and Y. Xia, *Adv. Mater.*, 2006, **18**, 1745.
14 J. Jin, X. Zhang, S. Nishimoto, Z. Liu, D. A. Tryk, T. Murakami and A. Fujishima, *Nanotechnology*, 2007, **18**, 075605.
15 (*a*) B. Lim, H. C. Camargo and Y. Xia, *Langmuir*, 2008, **24**, 10437; (*b*) K. H. Lee, S. C. Rah and S. J. Kim, *J. Sol-Gel Sci. Technol.*, 2008, **45**, 187.
16 R. Abargues, K. Abderrafi, E. Pedrueza, R. Gradess, J. Marqués-Hueso, J. Luis Valdés and J. Martínez-Pastora, *New J. Chem.*, 2009, **33**, 1720.
17 S. Kuo, C. Huang, C. Wu and F. Chang, *Polymer*, 2004, **45**, 6613.
18 S. Clémenson, L. David and E. Espuche, *J. Polym. Sci., Part A: Polym. Chem.*, 2007, **45**, 2657.